

Electronic Supplementary Information (ESI) for

Efficient and durable flexible perovskite photovoltaics with Ag embedded ITO as top electrode on metal substrate

Minoh Lee,^a Yimhyun Jo,^b Dong Suk Kim,^b Hu Young Jeong,^c and Yongseok Jun^{*d}

^a Department of Chemical Engineering, Ulsan National Institute of Science and Technology (UNIST), Ulsan 689-798, Republic of Korea.

^b KIER-UNIST Advanced Center for Energy, Korea Institute of Energy Research, Ulsan 689-798, Republic of Korea.

^c School of Materials Science and Engineering, Ulsan National Institute of Science and Technology (UNIST), Ulsan 689-798, Republic of Korea.

^d Department of Materials Chemistry and Engineering, Konkuk University, Seoul 143-701, Republic of Korea.
Tel: 02-450-0440; E-mail: yjun@konkuk.ac.kr

Experimental

Synthesis of CH₃NH₃I (MAI)

MAI was prepared by mixing 24 mL of methylamine (40% in methanol, TCI) and 10 mL of hydroiodic acid (57 wt% in water, Aldrich) in a 250 mL round bottomed flask at 0 °C for 2 h with stirring. The precipitate was obtained by drying at 50 °C for 30 min in rotary evaporator, which was dissolved in ethanol, recrystallized with diethyl ether. After air pump filtration, white product was finally dried at 60 °C in a vacuum oven for 24 h.

Device preparation

Ti foils (GoodFellow, 99.6 wt.% purity) were prepared in the form of ~15 × 15 × 0.127 mm³. Electro-polished Ti foil (~127 μm) was sequentially cleaned with ethanol, isopropanol, and distilled water. Subsequently, SiO₂ layer (~200 nm) by RF sputtering at deposition rate of 1.29 Å s⁻¹ with a RF power of 600 W and under 10 mTorr. And then, compact TiO₂ layer was deposited on Ti foil by spray pyrolysis, on a hotplate kept at 450°C. Approximately 300 nm thick mesoporous TiO₂ (mp-TiO₂) film was fabricated onto the TiO₂ dense layer/FTO substrate from a diluted commercial TiO₂ paste (1:4 with ethanol, w/w) by spin-coating, which was moved to a muffle furnace and sintered in air at 500°C for 30 min. The substrate was immersed in 40 mM TiCl₄ aqueous solution and kept at 70°C for 30 min in an oven, then transferred to a muffle furnace and annealed at 500°C for 15 min. After fabricating the TiO₂ film on the Ti substrate, it was moved into a nitrogen-filled glove box. Using 100 μL of the 1 M CH₃NH₃PbI₃ solution, the synthesized MAI powder was mixed with PbI₂ (Aldrich) in a mixture of *N,N*-dimethylformamide:*N*-Methyl-2-pyrrolidone (1:1, v/v). The solution was

dropped and spin-coated onto the mp-TiO₂/dense TiO₂/Ti substrate at 500 rpm for 5 s and 5000 rpm for 20 s. In final stage of spin-coating, 100 mL of toluene was dropped onto the center of the substrate, followed by annealing at 100 °C for 1 h. A hole transporting material (HTM) solution was prepared by dissolving 72.3 mg spiro-MeOTAD, 17.5 μL lithium bis(trifluoromethylsulphonyl)imide/acetonitrile (500 mg mL⁻¹), and 28.8 μL 4-tert-butylpyridine in 1 mL chlorobenzene. This solution was coated at 3000 rpm for 30 s. Finally, ~200 nm of ITO was deposited by DC sputtering at room temperature. The base pressure during sputter deposition was less than 5×10⁻⁶ Torr prior to the growth and the total working pressure was held constant at 1 mTorr. A sputtering power density of 150 W was employed during deposition. The gas flow rate (Ar 99,999%) was kept at 5 sccm. The active area was fixed at 0.135 cm². Perovskite solar cells on FTO-coated glass (Pilkington, TEC15) were also fabricated by the same procedure as above, except for the SiO₂ patterning. In addition, the Ag thin film was inserted prior to ITO sputtering, using thermal evaporation under < 10⁻⁶ Torr at rate of 0.2 Å s⁻¹.

Measurement and characterization

The crystal structure of the prepared films was investigated with an X-ray diffractometer (XRD, Bruker D8 Advance) equipped with Cu K α radiation. The absorbance spectra of the perovskite layer and the modified ITO film, and the transmittance of the ITO film were measured using a UV/Vis/NIR spectroscopy (Cary 5000, Agilent). The surface morphologies were characterized by field emission-scanning electron microscopy (FE-SEM, Nano230, FEI). Focused ion beam (Helios 450HP, FEI) milling was performed using a 30 kV ion beam for cross-sectional imagery. Energy dispersive X-Ray spectroscopy (EDX) characterization was performed with an EDX detector. The surface roughness and morphology of the prepared samples were investigated using tapping-mode atomic force microscopy. (AFM, Multimode V, Veeco). The sheet resistance of the prepared samples were measured using a hole effect measurement system (HMS-5500, Ecopia). The photocurrent density–voltage (*J*–*V*) curves of perovskite solar cells were measured using a Keithley 2400 digital source meter under the illumination of a solar simulator (AM 1.5 G, 100 mW cm⁻², Sol3A, class AAA, Oriel) as a light source with the calibrated light intensity to 1 sun using a reference Si solar cell (PV Measurements, Inc.). IPCE was measured by PV measurement equipped with a 75 W xenon lamp as a light source (PV Measurements, Inc.). Bending test performance of the devices was measured as a function of the number of bending cycles in an outward direction at a bending radius of ~6 mm.

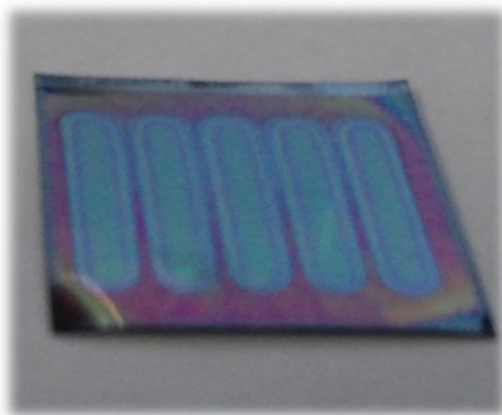
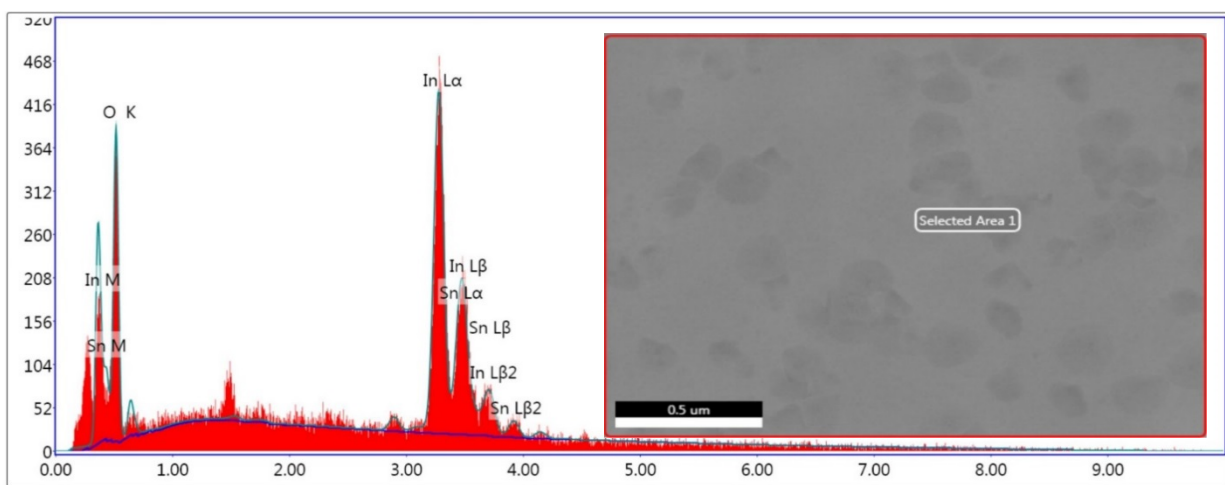


Fig. S1. Optical image of a perovskite solar cell on the Ti substrate using ITO as the top electrode.



Lsec: 29.5 0 Cnts 0.000 keV Det: Octane Plus Det

Fig. S2. EDX image of perovskite solar cells using ITO as the top electrode on the Ti substrate.

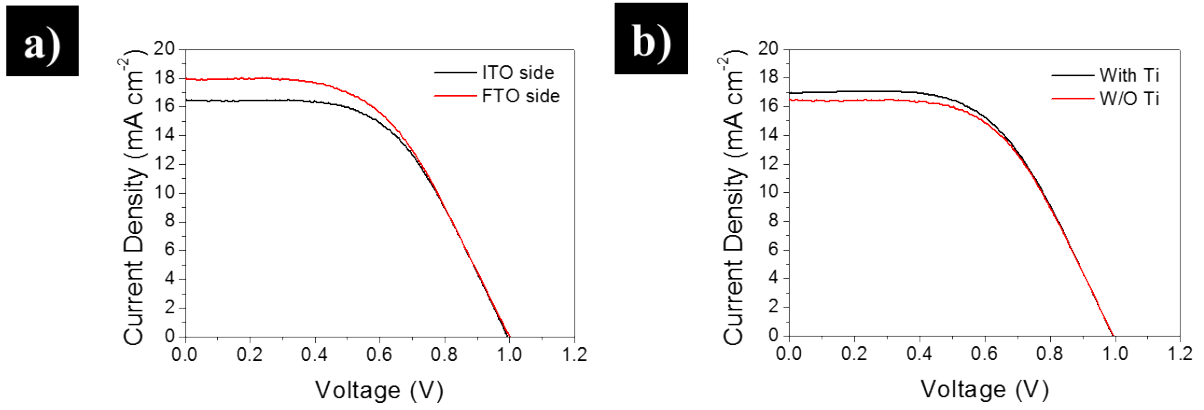


Fig. S3. (a) J - V curves of perovskite solar cells using ITO as the top electrode on the FTO glass substrate with ITO and FTO side illumination. (b) Effect of reflection by adding Ti substrate at the back of FTO glass side.

Table S1. Photovoltaic parameters of perovskite solar cells on glass substrate using ITO as top electrode with ITO and FTO side illumination. Devices measured under 100 mW cm⁻² simulated AM 1.5 G illumination.

		V_{oc} / V	$J_{sc} / \text{mA cm}^{-2}$	FF	PCE (%)
Front Illumination		0.999	17.9	53.1	9.50
Back Illumination	Without Ti	0.996	16.5	55.3	9.10
	With Ti	0.996	16.9	55.0	9.26

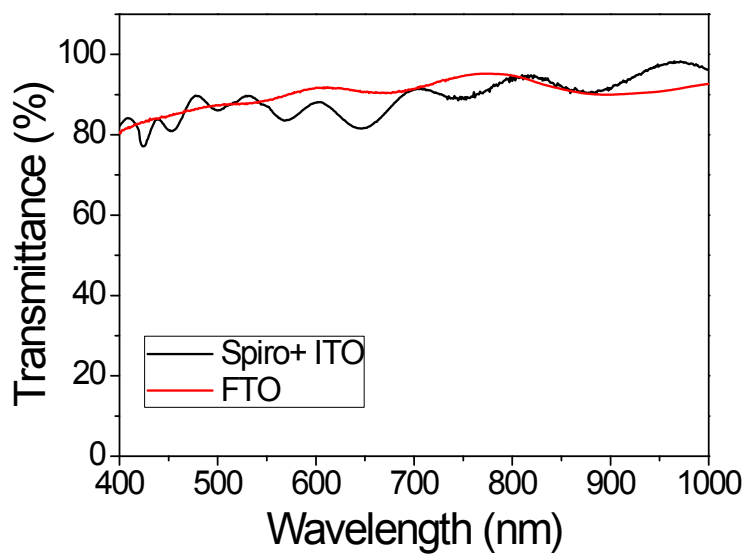


Fig. S4. Transmittance spectra of the ITO/spiro-MeOTAD/glass and FTO on glass.

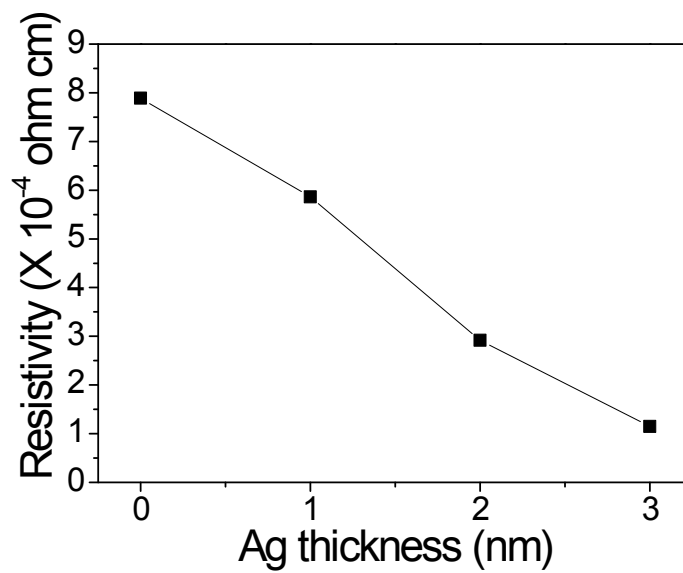


Fig. S5. Resistivity of ITO electrode as a function of Ag thickness.

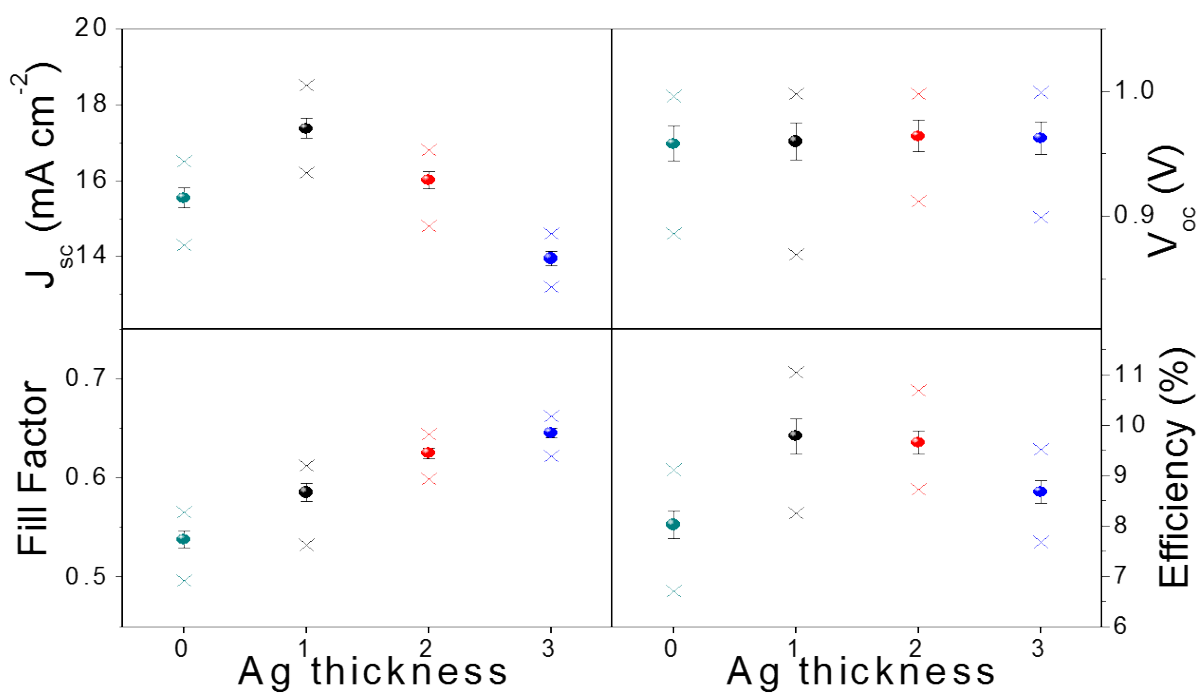


Fig. S6. Effect of Ag thin film insertion between spiro-MeOTAD and ITO for cathode in FPSCs. Mean device parameters extracted from J - V measurements for 16 devices with different Ag thin film thicknesses.

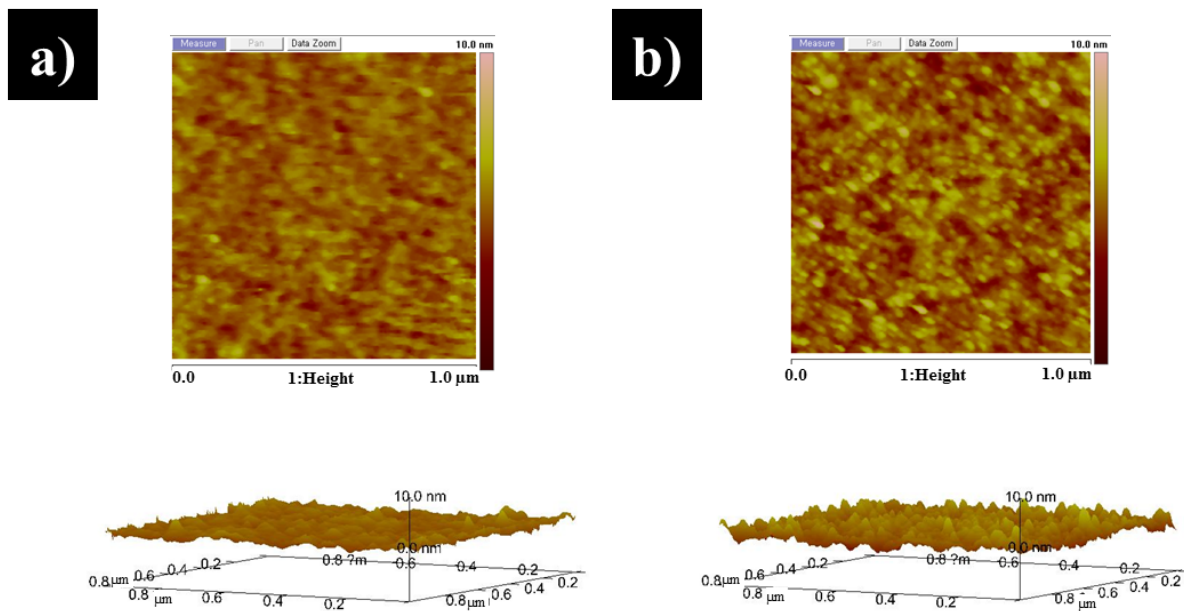


Fig. S7. AFM images of (a) spiro-MeOTAD on glass (b) 2nm of Ag deposited on spiro-MeOTAD/glass.

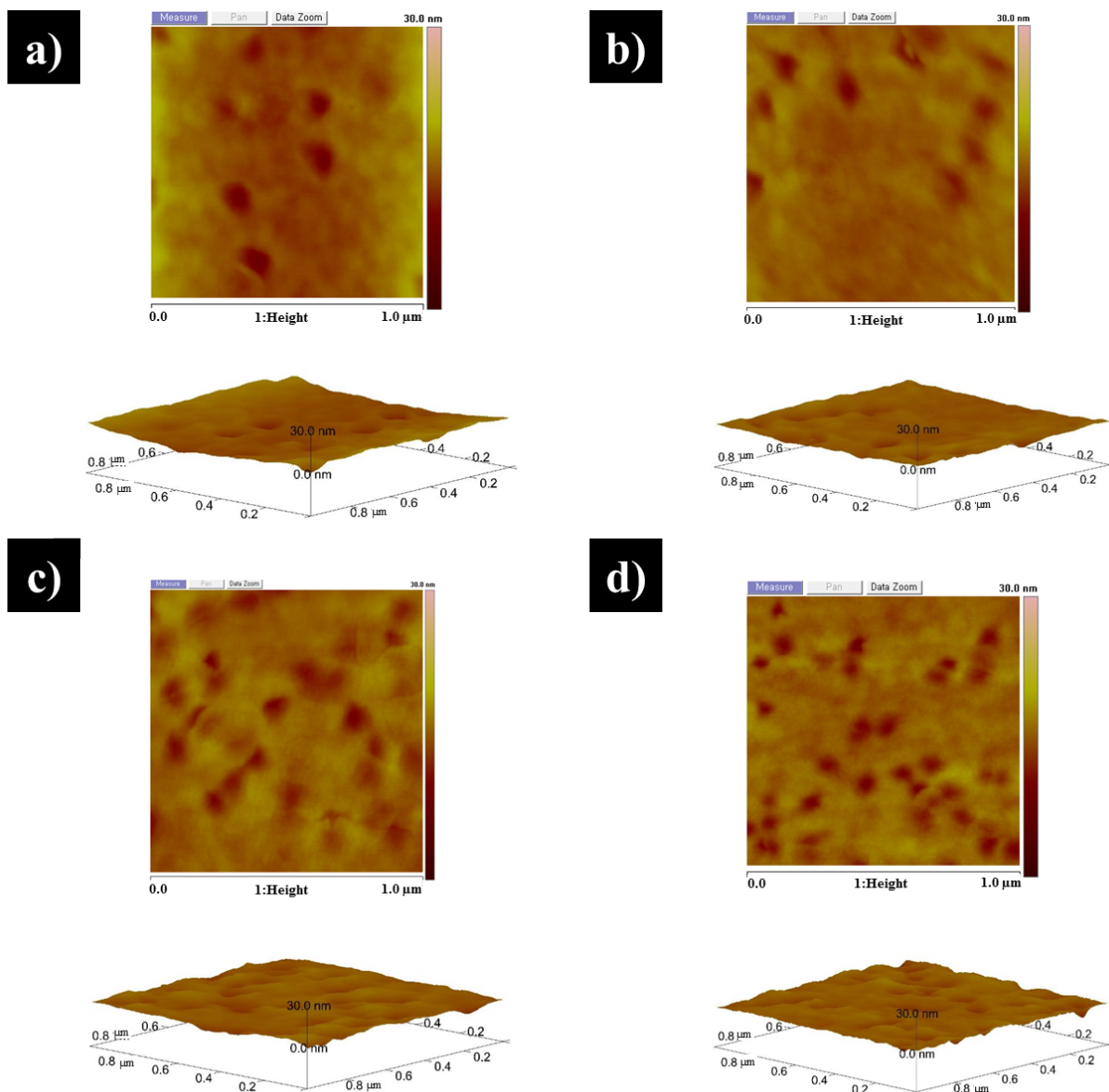


Fig. S8. AFM images of ITO film with different Ag thin film embedded between spiro-MeOTAD/glass and ITO layer. (a) 0 nm (b) 1nm (c) 2nm (d) 3nm.

To analyze the surface topography of the Ag-ITO electrodes, atomic force microscopy (AFM) was performed for different Ag thicknesses (Fig. S8a–S8d). The size of the AFM images is $1 \times 1 \mu\text{m}^2$. For the bare ITO electrode, a smoother morphology with a root-mean-square roughness (R_q) of 0.82 nm was observed, as shown Fig. S8a. However, R_q changes from 0.82 to 1.12 nm with increasing Ag thickness.

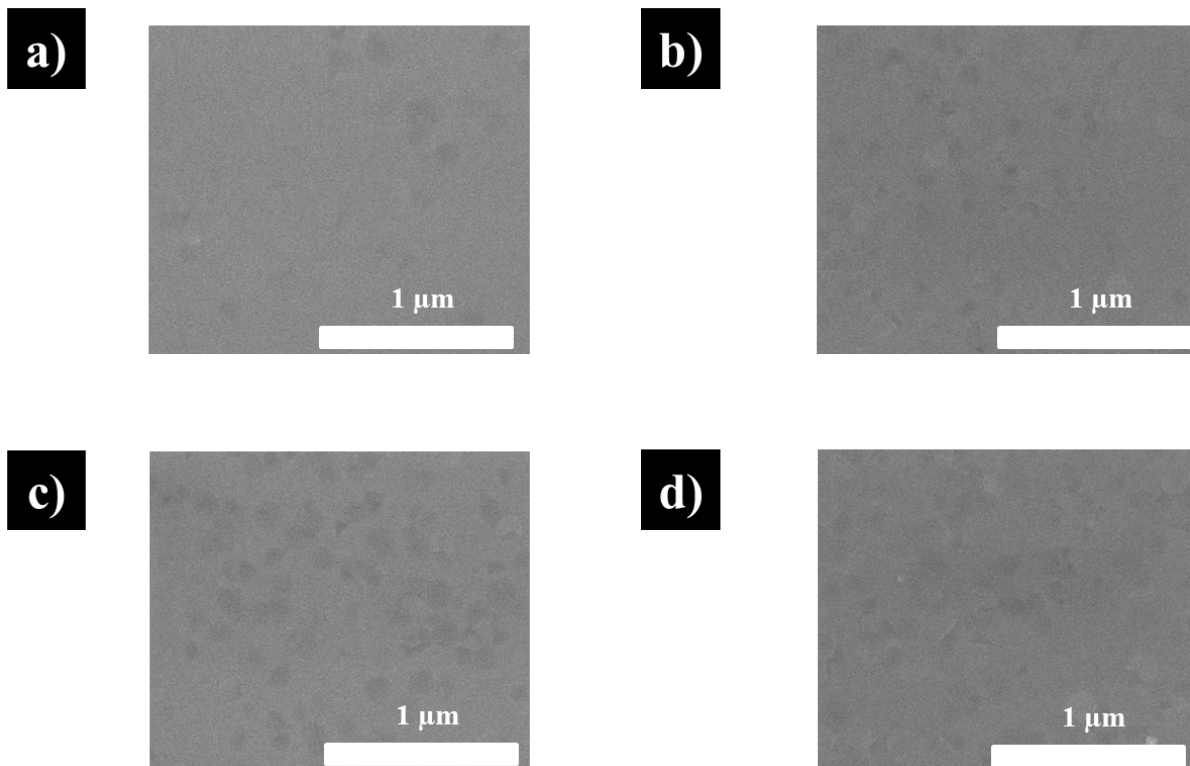


Fig. S9. SEM images of ITO film with different Ag film embedded between spiro-MeOTAD/glass and ITO layer. (a) 0 nm (b) 1nm (c) 2nm (d) 3nm.

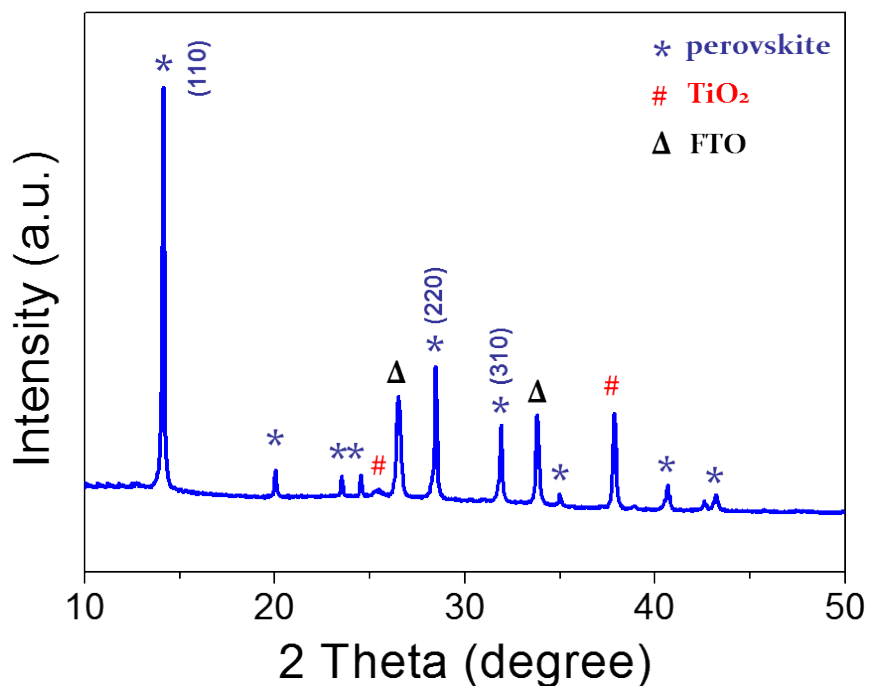


Fig. S10. XRD spectra of perovskite film on TiO_2/FTO glass after annealing at 100 °C.

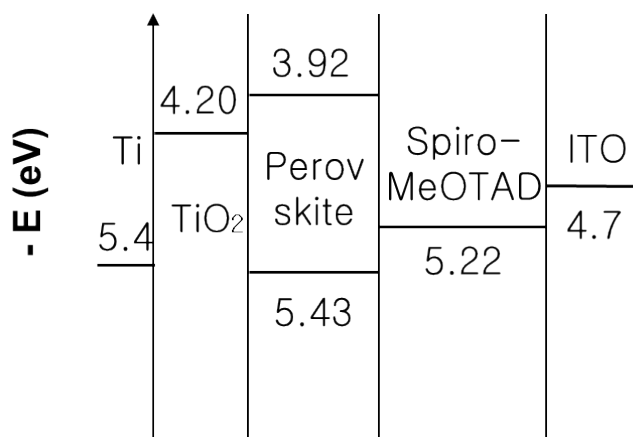


Fig. S11. Energy level diagram of FPSCs using ITO as the top electrode on the Ti substrate.

Energy level diagram of FPSCs using ITO top electrode is given in Fig. S11. Relatively low fill factor in devices are assumed due to energy level discrepancy between spiro-MeOTAD and ITO top electrode. ¹

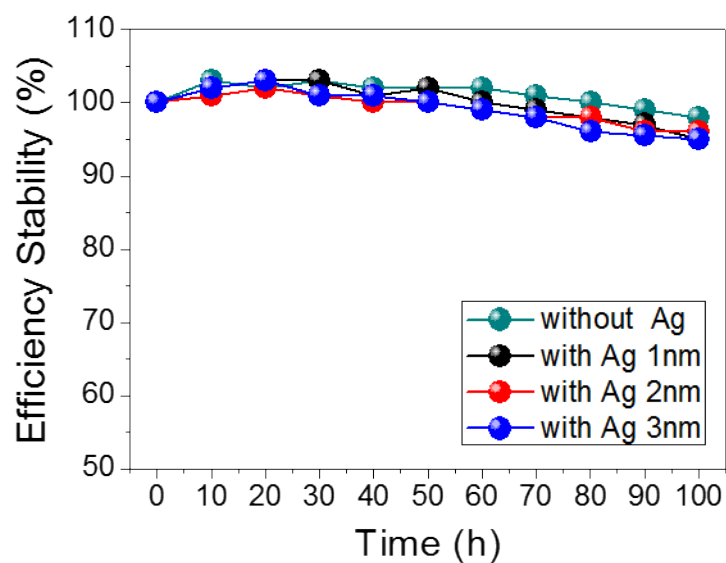


Fig. S12 Time evolution of efficiencies in photovoltaic.

Figure S12 shows the time evolution of efficiency in photovoltaics using ITO and Ag-ITO as top electrodes. Devices were stored in vacuum conditions for 100 h, over 95% of PCE from the initial value was retained for all devices.

Table S2 Photovoltaic parameters of perovskite solar cells on the Ti substrate using ITO as the top electrode with the insertion of varying thicknesses of Ag thin film with respect to scan direction (scan rate 20 mV s⁻¹).

Sample	Scan direction	V_{oc} / V	J_{sc} / mA cm ⁻²	FF (%)	PCE (%)
ITO	Forward	0.986	15.74	0.52	8.07
	Reverse	0.991	15.52	0.55	8.45
Ag 1 nm_ITO	Forward	0.987	17.56	0.56	9.70
	Reverse	0.991	17.38	0.59	10.16
Ag 2 nm_ITO	Forward	0.986	16.07	0.59	9.34
	Reverse	0.990	15.82	0.62	9.71
Ag 3 nm_ITO	Forward	0.987	13.91	0.63	8.64
	Reverse	0.990	13.75	0.65	8.84

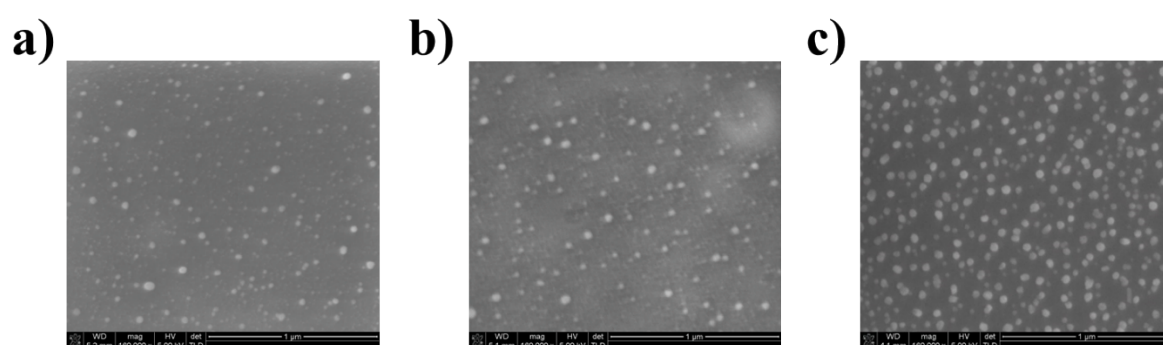


Fig. S13. SEM images of different thickness of Ag on spiro-MeOTAD. (a) 1 nm (b) 2 nm (c) 3 nm.

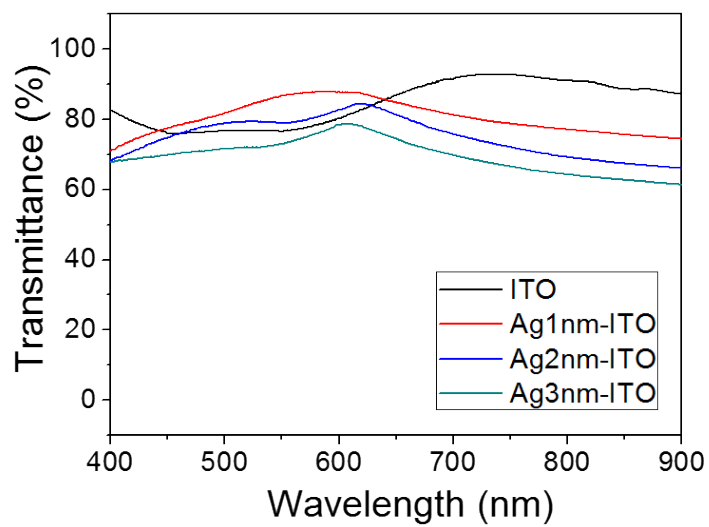


Fig. S14. Transmittance spectra of different thickness of Ag between spiro-MeOTAD and ITO.

Reference

1. G. Y. Margulis, M. G. Christoforo, D. Lam, Z. M. Beiley, A. R. Bowring, C. D. Bailie, A. Salleo and M. D. McGehee, *Advanced Energy Materials*, 2013, **3**, 1657-1663.